arXiv:astro-ph/0007221v2 4 Nov 2000

On the Origin of the Rotation Curves of Dark-Matter-Dominated Galaxies

Ilian T. Iliev

Department of Physics, University of Texas, Austin, 78712

iliev@astro.as.utexas.edu

and

Paul R. Shapiro

Department of Astronomy, University of Texas, Austin, 78712

shapiro@astro.as.utexas.edu

Received _____; accepted _____

Submitted to ApJ Letters

ABSTRACT

Rotation curves of dark-matter-dominated galaxies measure the mass profiles of galactic halos and thereby test theories of their cosmological origin. While attention has focused lately on the possible discrepancy at small galactocentric radii between observed rotation curves and the singular density profiles predicted by N-body simulations of the Cold Dark Matter (CDM) model, the observed rotation curves nevertheless contain valuable additional information with which to test the theory and constrain the fundamental cosmological parameters, despite this uncertainty at small radii. An analytical model we derived elsewhere for the postcollapse equilibrium of cosmological halos as truncated, nonsingular, isothermal spheres (TIS) reproduces many of the average properties of halos in CDM simulations to good accuracy, including the density profiles outside the central region. The circular velocity profile of this TIS model is, moreover, in excellent agreement with the observed ones and yields the mass and formation epoch of an observed halo from the parameters of its rotation curve. This allows us to predict correlations amongst rotation curve parameters, such as the maximum velocity and the radius at which it occurs, for different mass halos forming at different epochs in the CDM model. As an example, we derive the observed $v_{\rm max}$-$r_{\rm max}$ relation analytically, with preference for the flat ΛCDM model.

Subject headings: cosmology: theory – dark matter – galaxies: general – galaxies: formation – galaxies: halos – galaxies: kinematics and dynamics

1. Introduction

The rotation curves of dark-matter-dominated galaxies probe the mass profile of their galactic halos. The observed rotation curves of dwarf and low-surface-brightness (LSB) disk galaxies, therefore, offer a relatively direct test of theories of cosmological halo formation, free of the complicating effects of the dynamical coupling of dissipationless dark matter and dissipative baryonic matter which affect the mass profiles of baryon-dominated galaxies. Recently, attention has focused on the apparent conflict between the singular halo density profiles predicted by CDM N-body simulations and the observed rotation curves, which favor a flat-density core (cf. Moore et al. 1999). This has led to intense scrutiny of both the observations and the CDM model, primarily in one of three directions: improvement in the numerical resolving power of the CDM N-body simulations to determine better the logarithmic slope of the predicted density profiles at small radii (e.g. Moore et al. 1999), ideas for modifying the microscopic properties of the dark matter so as to retain the more successful aspects of the CDM model while flattening the halo density profiles at small radii (e.g. Davé et al. 2000, and references therein), and suggestions that the rotation curve data lack sufficient spatial resolution near the center to distinguish unambiguously between a density profile with a flat-density core and the singular profiles predicted by CDM N-body simulations (e.g. van den Bosch & Swaters 2000). Despite these uncertainties, a meaningful comparison between the data and predictions for the *global* properties of the rotation curves of dark-matter-dominated galaxies is possible which serves to test the CDM model and discriminate amongst different background cosmologies. To demonstrate this, we show how the mass and formation epoch of a halo can be extracted from its observed rotation curve, by application of an analytical model for halo formation which reproduces the empirical description of these rotation curves extremely well.

Burkert (1995) showed that the observed rotation curves of several dark-matter-dominated dwarf galaxies are consistent with a common density profile with a flat-density core, according to

$$\rho(r) = \frac{\rho_{0,\mathrm{B}}}{(r/r_{0,\mathrm{B}} + 1)(r^2/r_{0,\mathrm{B}}^2 + 1)}. \tag{1}$$

Kravtsov et al. (1998) found that the rotation curves for a larger sample which included both dwarf and LSB galaxies are well fit by a similar universal halo profile given by

$$\rho(r) = \frac{\rho_S}{(r/r_S)^\gamma (1 + (r/r_S)^\alpha)^{(\beta-\gamma)/\alpha}}, \tag{2}$$

with $(\alpha, \beta, \gamma) = (2, 3, 0.2)$, which is only slightly steeper than the Burkert profile in the core but shares the slope at large radii, where $\rho \propto r^{-3}$. The circular velocity profiles [i.e. $v(r) \equiv (GM[\leq r]/r)^{1/2}$] for equations (1) and (2) are virtually indistinguishable at all radii, even near the center, where $v \propto r^{1-\gamma/2}$, since $1 - \gamma/2 = 1$ or 0.9, respectively.

This contrasts with the halo profiles found by N-body simulations of the standard CDM model. The universal fitting formula for simulated halos reported by Navarro, Frenk, & White (1997; NFW) is equation (2) with $(\alpha, \beta, \gamma) = (1, 3, 1)$, while Moore et al. (1999) find $(\alpha, \beta, \gamma) = (1.5, 3, 1.5)$. However, the circular velocity profiles for these halos differ significantly from those implied by equations (1) and (2) only at very small radii where the uncertainties in the shape of the observed rotation curves currently makes discrimination difficult. In the meantime, equation (1) generally fits the data better than does the NFW profile even when the latter is also an acceptable fit.

The Burkert profile, then, continues to serve as a useful empirical description of the universal mass profiles of dark-matter-dominated galactic halos. We show here that the truncated, nonsingular isothermal sphere model we derived elsewhere (Shapiro, Iliev & Raga 1998, Paper I; Iliev & Shapiro 2000, Paper II) has a density profile for which the circular velocity profile is essentially indistinguishable from that of the Burkert profile and, as such, provides a theoretical motivation for the latter. The TIS model goes well beyond

the prediction of density profile and rotation curve, however, to provide the size, mass, velocity dispersion and collapse epoch of the halo, as well. This makes possible the further interpretation of observations of dark-matter-dominated galaxies for comparison with the predictions of various cosmological models. At the same time, the TIS model can be shown to reproduce many of the average properties of the halos found in simulations of the standard CDM model, outside of the innermost region where the TIS halo has a flat-density core, unlike the CDM halos. As a result, a comparison of the analytical TIS predictions with observed properties of galaxies also offers insight into the standard CDM model. Finally, if suggestions like the self-interacting dark matter proposal of Spergel & Steinhardt (2000) are correct, that CDM might be more "collisional" as a way to eliminate the central cusp of standard CDM halos, then our TIS solution will also apply to these models, to the extent that the halo relaxation process makes the final equilibrium approximately isothermal.

In § 2, we briefly summarize the relevant properties of the TIS model and present a simple analytical formula for it with which to fit an observed rotation curve. In § 3 we demonstrate the excellent agreement between the TIS model rotation curve and that implied by equation (1) and show how this allows us to deduce the total mass and collapse epoch of a given halo directly from the parameters of its observed rotation curve. In § 4, we describe how the dependence of the average formation epoch of a halo on its mass in the CDM model results in statistical correlations amongst the parameters of the observed rotation curves. As an example, we use this approach to derive analytically the known correlation between the maximum velocity of each rotation curve and the radius at which it occurs.

2. The Truncated Isothermal Sphere Model

The TIS model is a particular solution of the Lane-Emden equation (suitably modified when $\Lambda \neq 0$) which results from the collapse and virialization of a top-hat density perturbation (c.f. Paper I for Einstein-de Sitter [EdS] universe and Paper II for $\Omega_0 < 1$ and $\lambda_0 = 0$ or $1 - \Omega_0$). The size r_t and velocity dispersion σ_V are unique functions of the mass and redshift of formation of the object for a given background universe. While the Lane-Emden equation requires a straightforward numerical solution, Paper I provides a convenient analytical fitting formula,

$$\rho(r) = \rho_0 \left[\frac{A}{a^2 + \zeta^2} - \frac{B}{b^2 + \zeta^2} \right], \tag{3}$$

where $\zeta \equiv r/r_0$ and $(A, a^2, B, b^2) = (21.38, 9.08, 19.81, 14.62)$, accurate to within 3% over the full range $0 \leq \zeta \leq \zeta_t \approx 30$ for both the EdS case and most low-density models of interest (i.e. $\Omega_0 \geq 0.3$). [Note: Our definition of the core radius is $r_{0,\rm TIS} \equiv r_{\rm King}/3$, where $r_{\rm King}$ is the "King radius" defined in Binney & Tremaine (1987), p. 228.] Equation (3) can be integrated to yield an analytical fitting formula for the TIS rotation curve, as well, given by

$$\frac{v(r)}{\sigma_V} = \left\{ A - B + \frac{1}{\zeta} \left[bB \tan^{-1}\left(\frac{\zeta}{b}\right) - aA \tan^{-1}\left(\frac{\zeta}{a}\right) \right] \right\}^{1/2}, \tag{4}$$

where $\sigma_V = (4\pi G \rho_0 r_0^2)^{1/2}$. This fit has a fractional error less than 1% over the full range of radii $0 \leq r \leq r_t$ for all matter-dominated background models. With a nonzero cosmological constant, the circular velocity becomes $v(r) = (GM[\leq r]/r)^{1/2}[1 - 2\rho_\lambda/\rho(r)]^{1/2}$, where ρ_λ is the constant vacuum energy density associated with the cosmological constant. For cases of current interest for a flat universe with $\Lambda \neq 0$ (i.e. $\Omega_0 \geq 0.3$), equation (4) can still be used, however, since it departs from the exact solution only slightly in the outer halo (i.e. at $r \sim r_t$) for halos collapsing even as late as $z = 0$; the fractional error is less than 6% at all radii and less than 1% for $r \leq (2/3)r_t$.

The TIS model quantitatively reproduces the average structural properties of halos

found in CDM simulations to good accuracy, suggesting that it is a useful analytical approximation for halos which form from more realistic initial conditions. An exception to this agreement is the very inner profile, where the TIS has a uniform-density core instead of a central cusp. Our TIS predictions agree to astonishingly high accuracy (i.e. to of order 1%) with the cluster mass-radius and radius-temperature relationships and integrated mass profiles derived from detailed CDM simulations of X-ray cluster formation by Evrard, Metzler, and Navarro (1996). Apparently, these simulation results are not sensitive to our disagreement in the core. A direct comparison of the TIS and NFW mass profiles reveals a very close agreement (fractional deviation of less than $\sim 10\%$) at all radii outside of a few TIS core radii (i.e. about one King radius), for NFW concentration parameters $4 \lesssim c_{\rm NFW} \lesssim 7$.

3. Application to Galaxy Rotation Curves

The rotation curve for equation (1) is given by

$$\frac{v_{\rm B}(r)}{v_{*,\rm B}} = \left\{ \frac{\ln\left[(\zeta_B+1)^2(\zeta_B^2+1)\right] - 2\tan^{-1}(\zeta_B)}{\zeta_B} \right\}^{1/2}, \tag{5}$$

where $\zeta_B \equiv r/r_{0,\rm B}$ and $v_{*,\rm B} \equiv (\pi G \rho_{0,\rm B} r_{0,\rm B}^2)^{1/2}$. To compare our TIS directly with equation (1), we solve for the ratios $\rho_{0,\rm TIS}/\rho_{0,\rm B}$ and $r_{0,\rm TIS}/r_{0,\rm B}$ which minimize the χ^2 of the fit of equation (5) to equation (4) over radii from 0 to r_t. The result in Figure 1, with $\rho_{0,\rm TIS}/\rho_{0,\rm B} = 0.7790$ and $r_{0,\rm TIS}/r_{0,\rm B} = 0.3276$, shows extremely good agreement, with a fractional deviation below 10% from $0.01 r_t$ to r_t and below 4% over the range $r > 0.03 r_t \approx r_{0,\rm TIS}$. For the TIS, the maximum circular velocity and its location are $v_{\rm max,TIS} = 1.5867 \sigma_{\rm V,TIS}$ at $r_{\rm max,TIS} = 8.99 r_{0,\rm TIS}$ for all matter-dominated cosmologies. For a flat universe with $\Lambda \neq 0$, ($\Omega_0 \geq 0.3$), these numbers depend weakly upon collapse redshift, but are reduced by no more than 0.2% and 1.7%, respectively, for $z_{\rm coll} = 0$, and by even less for earlier collapse. For the Burkert profile, $v_{\rm max,B} = 1.2143 v_{*,\rm B}$ at $r_{\rm max,B} = 3.2446\, r_{0,\rm B}$.

Hence, our best fit finds that $v_{\rm max}$ and $r_{\rm max}$ for the TIS and Burkert profiles are extremely close, with $v_{\rm max,TIS}/v_{\rm max,B} = 1.02$ and $r_{\rm max,TIS}/r_{\rm max,B} = 0.91$.

In short, our TIS model provides a solid, theoretical underpinning for the empirical fitting formula of Burkert, and, by extension, a self-consistent theoretical explanation of the observed galaxy rotation curves it was invented to fit. In addition, the TIS model allows us to calculate the total mass M_0, collapse epoch $z_{\rm coll}$, and other parameters of each observed dark-matter-dominated halo from its rotation curve, as follows. Assuming $v_{\rm max}$ and $r_{\rm max}$ are provided by observation[1], the mass of the galaxy can be shown to be

$$\frac{M_0}{h^{-1}M_\odot} = 6.329 \times 10^{10} \left(\frac{r_{\rm max}}{10\,h^{-1}\,{\rm kpc}}\right) \left(\frac{v_{\rm max}}{100\,{\rm km\,s^{-1}}}\right)^2 \tag{6}$$

for any matter-dominated universe. When $\Lambda \neq 0$, $M_0 \propto r_{\rm max} v_{\rm max}^2$, but the coefficient depends on $z_{\rm coll}$ and background cosmology (Paper II). For any flat universe ($\Lambda \neq 0$) of current interest, equation (6) is still a very good approximation. For $\Omega_0 = 1 - \lambda_0 \geq 0.3$, equation (6) underestimates the mass by less than 6.3%, 2.8%, and 1.2% for $z_{\rm coll} = 0, 0.5$, and 1, respectively.

In terms of $r_{\rm max}$ and $v_{\rm max}$, $z_{\rm coll}$ is given to good accuracy by the implicit equation

$$F(\Omega_0, \lambda_0, z_{\rm coll}) = 2.284 \left(\frac{v_{\rm max}/100\,{\rm km\,s^{-1}}}{r_{\rm max}/10\,h^{-1}\,{\rm kpc}}\right)^{2/3} \tag{7}$$

where $F \equiv \{[\Omega_0/\Omega(z_{\rm coll})][\Delta_{\rm c,SUS}/18\pi^2]\}^{1/3}(1+z_{\rm coll})$, $\Omega(z) = [\Omega_0(1+z)^3]/[(1-\Omega_0-\lambda_0)(1+z)^2 + \Omega_0(1+z)^3 + \lambda_0]$, and $\Delta_{\rm c,SUS}$ is the density [in units of $\rho_{\rm crit}(z_{\rm coll})$] after top-hat collapse and virialization for the standard uniform sphere approximation (SUS)[2]. For the EdS case,

[1]In practice, observations are generally restricted to the inner parts of galaxy rotation curves, often not extending to radii as large as $r_{\rm max}$. In that case, $v_{\rm max}$ and $r_{\rm max}$ are inferred by fitting the observed rotation curve to the TIS rotation curve at other radii.

[2]This $\Delta_{\rm c,SUS}$ is well-approximated by $\Delta_{\rm c,SUS} = 18\pi^2 + c_1 x - c_2 x^2$, where $x \equiv \Omega(z_{\rm coll}) - 1$,

$F = (1 + z_{\rm coll})$, while for open, matter-dominated and flat cases, $F \rightarrow \Omega_0^{-1/3}(1 + z_{\rm coll})$ at early times [i.e. $x \rightarrow 0$]. The coefficient on the r.h.s. of equation (7) is correct for any matter-dominated cosmology and a very good approximation for flat ($\Lambda \neq 0$) cases of current interest. For $\Omega_0 \geq 0.3$, it underestimates $(1 + z_{\rm coll})$ by less than 2.5% for $z_{\rm coll} \geq 0$.

4. Statistical Correlations Amongst the Properties of Dwarf and LSB Galaxies: The $v_{\rm max}$–$r_{\rm max}$ Relation

The halos in our TIS model are fully described for a given background universe by their total mass M_0 and collapse epoch $z_{\rm coll}$. In hierarchical models of structure formation like CDM, these are not statistically independent parameters, however. Smaller mass halos on average collapse earlier and are denser than larger mass halos. In terms of galaxy rotation-curve parameters, this dependence should be observable, for example, as a correlation between $v_{\rm max}$ and $r_{\rm max}$. Mori & Burkert (2000) used the Burkert (1995) fits to rotation curves of dwarf galaxies to report such an observed correlation, expressed as follows:

$$v_{\rm max,B} = 9.81\,(r_{\rm max,B}/1\,{\rm kpc})^{2/3}\ {\rm km\,s^{-1}}. \tag{8}$$

Kravtsov et al. (1998) also found a correlation using fits to observed rotation curves. Their results for a sample of dwarf and LSB galaxies are shown in Figure 2, along with that in equation (8). Kravtsov et al. (1998) further showed that the results of their CDM N-body simulations agreed with these data points.[3] This suggests that if we can relate the mass and

---

and $c_1 = 82\,(60)$ and $c_2 = 39\,(32)$ for the flat (open) cases, $\Omega_0 + \lambda_0 = 1$ ($\Omega_0 < 1, \lambda_0 = 0$), respectively (Bryan & Norman 1998).

[3]This result by Kravtsov et al. (1998) is not sensitive to the question of whether their simulations adequately resolved the halo density profiles at very small radii.

collapse epoch of our TIS model halos in a statistical way within the context of the CDM model, a comparison of our predicted $v_{\rm max}$-$r_{\rm max}$ relation with this observed one will further check the relevance of our TIS model to halo formation from realistic initial conditions and, at the same time, give a theoretical explanation for both the data and the simulation results.

To predict the $v_{\rm max}$–$r_{\rm max}$ correlation for a CDM universe using our TIS model, we apply the well-known Press-Schechter (PS) approximation to derive $z_{\rm coll}(M_0)$ - the typical collapse epoch for a halo with a given mass. Halos of mass M which collapse when $\sigma(M) = \delta_{\rm crit}/\nu$ are referred to as "ν-σ" fluctuations, where $\sigma(M)$ is the standard deviation of the density fluctuations at $z_{\rm coll}$ according to linear perturbation theory, after the density field is filtered on the scale M, and $\delta_{\rm crit}$ is the amplitude of a top-hat perturbation according to linear theory at the epoch $z_{\rm coll}$ at which the exact solution predicts infinite collapse. The typical collapse epoch for halos of a given mass is that for which $\nu = 1$, the 1-σ fluctuations.

Our results for 1-σ fluctuations are shown in Figure 2 (upper panel), for different background cosmologies. The flat, untilted and the open, slightly-tilted ($n_p = 1.14$) models are in reasonable agreement with the observed $v_{\rm max} - r_{\rm max}$ relation, while the untilted and strongly tilted ($n_p = 1.3$) open models are not. The empirical Burkert scaling relation is closely approximated by the currently-favored ΛCDM model, less well by other models.

In practice, observed galaxies should exhibit a statistical spread of halo properties in accord with the expectations of the Gaussian statistics of the density fluctuations which formed them. Since observed galaxies will not all be "typical", the scatter of the data points in Figure 2 is natural. To probe this in our model, we calculate the masses and collapse redshifts for halos formed by ν-σ fluctuations for different values of ν. As shown in Figure 2 (lower panel) for ΛCDM, the Burkert scaling relation is closest to the TIS model prediction for 1-σ fluctuations, while all the observed galaxy data points except one correspond to

$0.7 \lesssim \nu \lesssim 1.5$. Hence, on average, the galaxies which constitute the observed $v_{\rm max}$-$r_{\rm max}$ correlation correspond to halos which formed at close to the typical collapse time expected theoretically for objects of that mass. This means that our TIS model is a self-consistent explanation for the observed $v_{\rm max}$-$r_{\rm max}$ correlation.

This success of the TIS model in explaining the observed $v_{\rm max}$-$r_{\rm max}$ relation and, by extension, the CDM simulation results of Kravtsov et al. (1998) which follow it can be understood by a completely analytical argument, as follows. We approximate the density fluctuation power spectrum as a power-law in wavenumber k, $P(k) \propto k^n$. If we define a mass M which corresponds to k according to $M \propto k^{-3}$, then $\sigma(M) \propto M^{-(3+n)/6}$ if we set $n = n_{\rm eff} \equiv -3(2y_{\rm eff} + 1)$, where $y_{\rm eff} \equiv (d\ln\sigma/d\ln M)_{\rm exact}$ at the relevant mass scale M. Our results for the ΛCDM case indicate that the galaxies which make up the $v_{\rm max} - r_{\rm max}$ data points in Figure 2 collapsed at redshifts $1 \lesssim z_{\rm coll} \lesssim 6$ with masses in the range $8 \times 10^9 \lesssim M_0/(M_\odot h^{-1}) \lesssim 3 \times 10^{11}$. Hence, the precollapse fluctuation growth rate is approximately EdS, and we can let $\Omega(z_{\rm coll}) = 1$ in equations (6) and (7). In that case, $(1 + z_{\rm coll}) \propto \sigma(M) \propto M^{-(3+n)/6}$, $r_{\rm max} \propto M^{(5+n)/6}\Omega_0^{-1/3}$ and $v_{\rm max} \propto M^{(1-n)/12}\Omega_0^{1/6}$, which combine to yield

$$v_{\rm max} = v_{\rm max,*}\,(r_{\rm max}/r_{\rm max,*})^{(1-n)/[2(5+n)]}, \tag{9}$$

where $v_{\rm max,*}$ and $r_{\rm max,*}$ are for a 1-σ fluctuation of fiducial mass M_*, as given by equations (6) and (7) with $(1 + z_{\rm coll}) = (1 + z_{\rm rec})\sigma(M_*, z_{\rm rec})/\delta_{\rm crit}$, where $\delta_{\rm crit} = 1.6865$ and $\sigma(M_*, z_{\rm rec})$ is the value of $\sigma(M_*)$ evaluated at the epoch of recombination $z_{\rm rec}$ [i.e. early enough that $(1 + z)\sigma$ is independent of z]. Over the relevant mass range $M = 10^{10\pm1}h^{-1}M_\odot$, $n_{\rm eff} \approx -2.4 \pm 0.1$ for our ΛCDM case. For $M_* = 10^{10}h^{-1}M_\odot$, our COBE-normalized, flat ΛCDM case ($\Omega_0 = 0.3, h = 0.65$) yields $(1 + z_{\rm rec})\sigma(M_*, z_{\rm rec}) = 5.563$, so $(1 + z_{\rm coll}) = 3.30$, $v_{\rm max,*} = 53.2\,{\rm km\,s^{-1}}$ and $r_{\rm max,*} = 5.59\,h^{-1}{\rm kpc}$. With these values and $n_{\rm eff} = -2.4$, equation (9) yields the TIS model analytical prediction $v_{\rm max} = (13.0\,{\rm km\,s^{-1}})(r_{\rm max}/1\,{\rm kpc})^{0.65}$, remarkably close to the empirical relation in equation (8).

We thank Hugo Martel for valuable discussion, grants NASA ATP NAG5-7363 and NAG5-7821, NSF ASC-9504046, and Texas Advanced Research Program 3658-0624-1999, and an NSF International Research Fellow Award INT-0003682 to ITI.

REFERENCES

Bryan, G.L. & Norman, M.L. 1998, ApJ, 495, 80

Burkert, A. 1995, ApJ, 447, L25

Davé R., Spergel, D.N., Steinhardt, P.J., & Wandelt, B.D. 2000, ApJ, submitted (astro-ph/0006218)

Iliev, I.T. & Shapiro, P.R. 2000, to be submitted (Paper II)

Kravtsov, A.V., Klypin, A.A., Bullock, J.S., & Primack, J.R. 1998, ApJ, 502, 48

Moore, B., Quinn, T., Governato, F., Stadel, J., & Lake, G. 1999, MNRAS, 310, 1147

Mori, M. & Burkert, A. 2000, ApJ, 538, 559

Navarro, J.F., Frenk, C.S., & White, S.D.M. 1997, ApJ, 490, 493

Shapiro, P.R., Iliev, I.T., & Raga, A.C. 1999, MNRAS, 307, 203 (Paper I)

Spergel, D.N. & Steinhardt, P.J. 2000, Phys.Rev.Lett., 84, 17

van den Bosch, F.C. & Swaters, R.A. 2000, preprint (astro-ph/0006048)

Fig. 1.— Circular velocity profiles $v(r)$ (in units of $\sigma_{V,TIS}$) versus radius r (in units of $r_{0,TIS}$) for the TIS model halo (matter-dominated universe)(solid line) and for the best-fit Burkert (1995) profile (dotted line), fit over the entire range $0 \leq r \leq r_t$ (i.e. $0 \leq \zeta \leq \zeta_t \approx 30$). Top panel shows the fractional deviation $(v_{\rm TIS} - v_B)/v_{\rm TIS}$.

This manuscript was prepared with the AAS LaTeX macros v5.0.

Fig. 2.— (a) (upper panel) $v_{\rm max}$–$r_{\rm max}$ correlation. Observed dwarf galaxies (triangles) and LSB galaxies (squares) from Kravtsov et al. (1998). Curve labelled "Burkert fit" is equation (8) based on a fit by Burkert (1995) to data. TIS+PS predictions are plotted for different CDM cosmologies, as labelled: SCDM ($\Omega_0 = 1$, cluster-normalized: $\sigma_{8{\rm h}^{-1}} = 0.5$), OCDM ($\Omega_0 = 0.3$, $\lambda_0 = 0$, COBE-normalized, both untilted [primordial power spectrum index $n_p = 1$] and tilted [$n_p = 1.14$ and 1.3] (subscripts indicate n_p-value); and ΛCDM ($\Omega_0 = 1-\lambda_0 = 0.3$, COBE-normalized). In the untilted ΛCDM and strongly-tilted ($n_p = 1.3$) open cases, COBE- and cluster-normalizations are the same. All models assume $h = 0.65$. (b) (lower panel) Same as (a), except TIS+PS curves are for the ΛCDM model only, for fluctuations of different initial amplitudes for each mass scale, as labelled by the "ν-σ" values: 1-σ (i.e. "typical" fluctuations), 0.5-σ,0.7-σ,1.5-σ, and 2-σ.

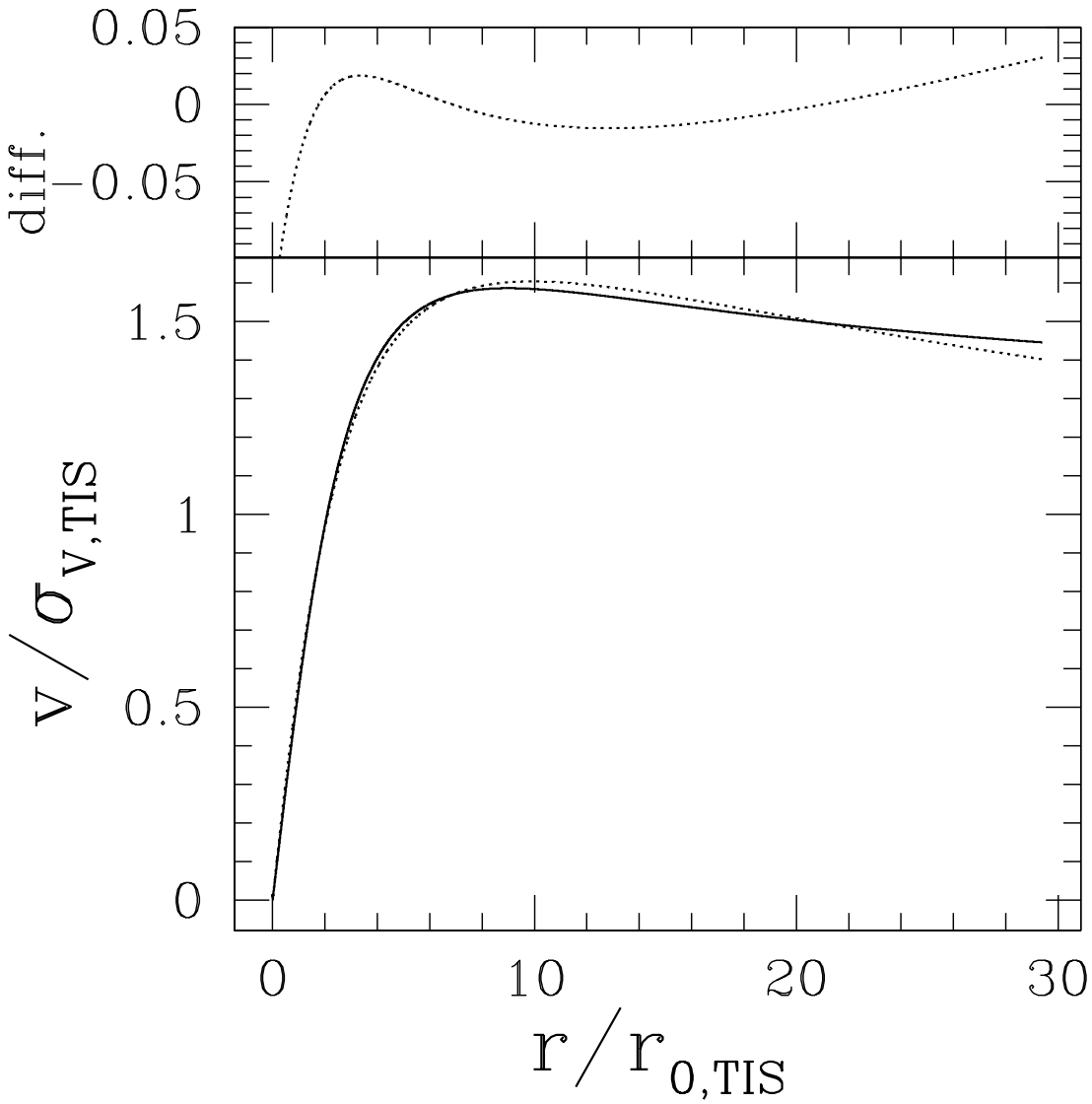
0.05
0
−0.05
diff.
1.5
1
0.5
0
v / σ v,TIS
0
10
20
30
r / r 0,TIS

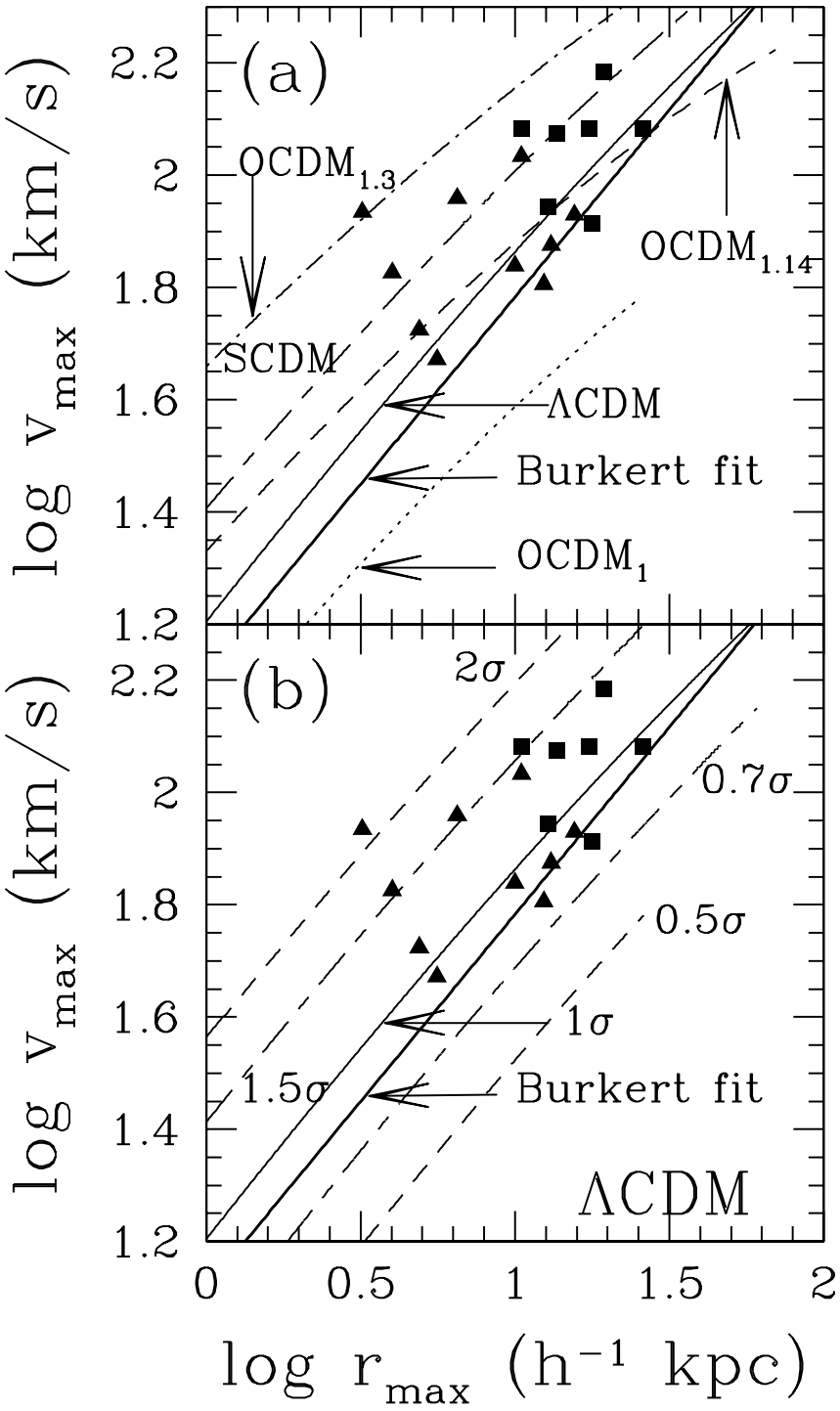
(a)
OCDM1.3
OCDM1.14
SCDM
ΛCDM
Burkert fit
OCDM1
(b)
2σ
0.7σ
0.5σ
1σ
1.5σ
Burkert fit
ΛCDM
log vmax (km/s)
log rmax (h−1 kpc)
1.2
1.4
1.6
1.8
2
2.2
0
0.5
1
1.5
2